Rapid X-ray flaring from the direction of the supermassive black hole at the Galactic Centre

F. K. Baganoff*, M. W. Bautz*, W. N. Brandt†, G. Chartas†, E. D. Feigelson†, G. P. Garmire†, Y. Maeda†‡, M. Morris§, G. R. Ricker*, L. K. Townsley† & F. Walter‖

** Center for Space Research, Massachusetts Institute of Technology, Cambridge, Massachusetts 02139-4307, USA*
† Department of Astronomy and Astrophysics, Pennsylvania State University, University Park, Pennsylvania 16802-6305, USA
‡ Institute of Space and Astronautical Science, 3-1-1 Yoshinodai, Sagamihara, 229-8501, Japan
§ Department of Physics and Astronomy, University of California at Los Angeles, Los Angeles, California 90095-1562, USA
‖ Department of Astronomy, California Institute of Technology, Pasadena, California 91125, USA

The nuclei of most galaxies are now believed to harbour supermassive black holes[1]. The motions of stars in the central few light years of our Milky Way Galaxy indicate the presence of a dark object with a mass of about 2.6×10^6 solar masses (refs 2, 3). This object is spatially coincident with the compact radio source Sagittarius A* (Sgr A*) at the dynamical centre of the Galaxy, and the radio emission is thought to be powered by the gravitational potential energy released by matter as it accretes onto a supermassive black hole[4,5]. Sgr A* is, however, much fainter than expected at all wavelengths, especially in X-rays, which has cast some doubt on this model. The first strong evidence for X-ray emission was found only recently[6]. Here we report the discovery of rapid X-ray flaring from the direction of Sgr A*, which, together with the previously reported steady X-ray emission, provides compelling evidence that the emission is coming from the accretion of gas onto a supermassive black hole at the Galactic Centre.

Our view of Sgr A* in the optical and ultraviolet wavebands is blocked by the large visual extinction, $A_V \approx 30$ magnitudes[7], caused by dust and gas along the line of sight. Sgr A* has not been detected in the infrared owing to its faintness and to the bright infrared background from stars and clouds of dust[8]. We thus need to detect X-rays from Sgr A* in order to constrain the spectrum at energies above the radio-to-submillimetre band and to test whether gas is accreting onto a supermassive black hole (see above).

We first observed the Galactic Centre on 21 September 1999 with the imaging array of the Advanced CCD (charge-coupled device) Imaging Spectrometer (ACIS-I) aboard the Chandra X-ray Observatory[9] and discovered an X-ray source coincident within $0.35'' \pm 0.26''$ (1σ) of the radio source[6]. The luminosity in 1999 was very weak—$L_X \approx 2 \times 10^{33}$ erg s^{-1} in the 2–10 keV band—after correction for the inferred neutral hydrogen absorption column $N_H \approx 1 \times 10^{23}$ cm^{-2}. This is far fainter than previous X-ray observatories could detect[6].

We observed the Galactic Centre a second time with Chandra ACIS-I from 26 October 2000 22:29 until 27 October 2000 08:19 (UT), during which time we saw a source at the position of Sgr A* brighten dramatically for a period of approximately 10,000 s (10 ks). Figure 1 shows surface plots for both epochs of the 2–8 keV counts integrated over time from a $20'' \times 20''$ region centred on the radio position of Sgr A*. The modest peak of the integrated counts at Sgr A* in 1999 increased by a factor of about 7 in 2000, despite the 12% shorter exposure. The peak integrated counts of the fainter features in the field show no evidence of strong variability, demonstrating that the flaring at Sgr A* is intrinsic to the source.

Figure 2 shows light curves of the photon arrival times from the direction of Sgr A* during the observation in 2000. Figure 2a and b shows hard-band (4.5–8 keV) and soft-band (2–4.5 keV) light curves constructed from counts within an angular radius of 1.5″ of Sgr A*. Both bands exhibit roughly constant, low-level emission for the first 14 ks or so, followed by a 6-ks period of enhanced emission beginning with a 500-s event (4.4σ significance using 150-s bins). At 20 ks, flare(s) of large relative amplitude occur, lasting about 10 ks, and finally the emission drops back to the low state for the remaining 6 ks or so. About 26 ks into the observation, the hard-band light curve drops abruptly by a factor of 5 within a span of around 600 s and then partially recovers within a period of 1.2 ks. The soft-band light curve shows a similar feature, but it appears to lag the hard-band event by a few hundred seconds and is less sharply defined.

The band-ratio time series in Fig. 2c, defined as the ratio of hard-band counts to soft-band counts, suggests that the spectrum 'hardened' (that is, became flatter and extended more strongly to higher energies) during the flare. The difference between the band ratio measured at the peak of the flare and the average of the band ratios during the quiescent periods at the beginning and end of the observation is 0.63 ± 0.21 (that is, 3σ). The peak-flare band ratio in Fig. 2c is affected to some extent by the effects of pile-up (see Fig. 2 legend), which would tend to harden the spectrum; however, the band ratios in Fig. 2d, which were computed using the non-piled-up data extracted from the wings of the point spread function, also show evidence for spectral hardening with 2.7σ significance. The sizes of dust-scattering haloes in the Galactic Centre are typically

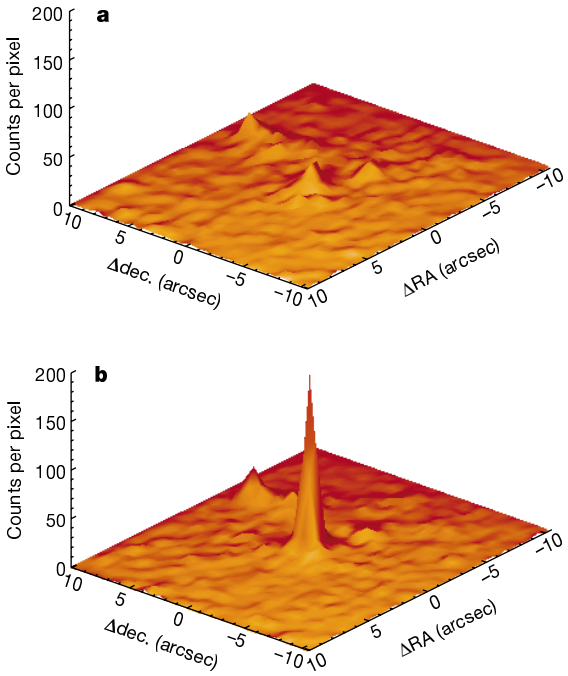

Figure 1 Surface plots of the 2–8 keV counts within a $20'' \times 20''$ field centred on Sgr A* at two epochs. The data were taken with Chandra ACIS-I on (**a**) 21 September 1999 and (**b**) 26–27 October 2000. The effective exposure times were 40.3 ks and 35.4 ks, respectively. The spatial resolution is 0.5″ per pixel. An angle of 1″ on the sky subtends a projected distance of about 0.04 pc at the galactocentric distance of 8.0 kpc (ref. 30). The peak integrated counts per pixel at the position of Sgr A* increased by a factor of 7 from the first epoch to the second, despite the slightly smaller exposure time (~12%) in the second epoch. The low-level peak a few arcseconds to the southwest of Sgr A* is the infrared source IRS 13, and the ridge of emission to the northwest is from a string of unresolved point sources. The fainter features in the field are reasonably consistent between the two epochs, considering the limited Poisson statistics and the fact that these stellar sources may themselves be variable; this consistency shows that the strong variations at Sgr A* are intrinsic to the source.

greater than 1′ (ref. 10), so dust-scattered X-rays from the source contribute a negligible fraction of the emission within the source extraction region that we used; hence dust-scattered X-rays cannot account for the spectral variations. We therefore conclude that the spectral hardening during the flare is likely to be real.

The quiescent-state spectra in 1999 and 2000 and the peak flaring-state spectrum in 2000 are shown in Fig. 3. We fitted each spectrum individually using a single power-law model with corrections for the effects of photoelectric absorption and dust scattering[10]. The best-fit values and 90% confidence limits for the parameters of each fit are presented in the first three lines of Table 1. The column densities for the three spectra are consistent, within the uncertainties, as are the photon indices of both quiescent-state spectra. Next, we fit a double power-law model to the three spectra simultaneously, using a single photon index for both quiescent spectra, a second photon index for the flaring spectrum, and a single column density for all three spectra. The best-fit models for each spectrum from the simultaneous fits are shown as solid lines in Fig. 3; the parameter values are given in the last line of Table 1. Using these values, we derive an absorption-corrected 2–10 keV luminosity of $L_X = (2.2^{+0.4}_{-0.3}) \times 10^{33}$ erg s^{-1} for the quiescent-state emission and $L_X = (1.0 \pm 0.1) \times 10^{35}$ erg s^{-1} for the peak of the flaring-state emission, or around 45 times the quiescent-state luminosity. We note that previous X-ray observatories did not have the sensitivity to detect such a short-duration, low-luminosity flare in the Galactic Centre[6]. The best-fit photon index $\Gamma_f = 1.3^{+0.5}_{-0.6}$ ($N(E) \propto E^{-\Gamma}$) for the flaring-state spectrum is slightly flatter than, but consistent with, systems thought to contain supermassive black holes[11]. Here E is the energy of a photon in keV, $N(E)$ is the number of photons with energies in the differential interval E to $E + dE$, and Γ is the power-law index of the photon number distribution.

If we view the outburst as a single event, the rise/fall timescales of a few hundred seconds and the 10-ks duration are consistent with the light-crossing and dynamical timescales for the inner part (at less than 10 Schwarzchild radii; $R_S \equiv 2GM/c^2$) of the accretion flow around a black hole of 2.6×10^6 solar masses ; here R_S is the radius of the black-hole event horizon (that is, the boundary at which the escape velocity equals the speed of light, c), G is the gravitational constant and M is the mass of the black hole. Although we cannot strictly rule out an unrelated contaminating source as the origin of the flare (for example, an X-ray binary, for which little is known about such short-timescale, low-luminosity events as we have detected; W. Lewin, personal communication), this explanation seems unlikely, as the characteristic angular scales of the young and old stellar clusters around Sgr A* are 5–20″ (ref. 7), whereas the

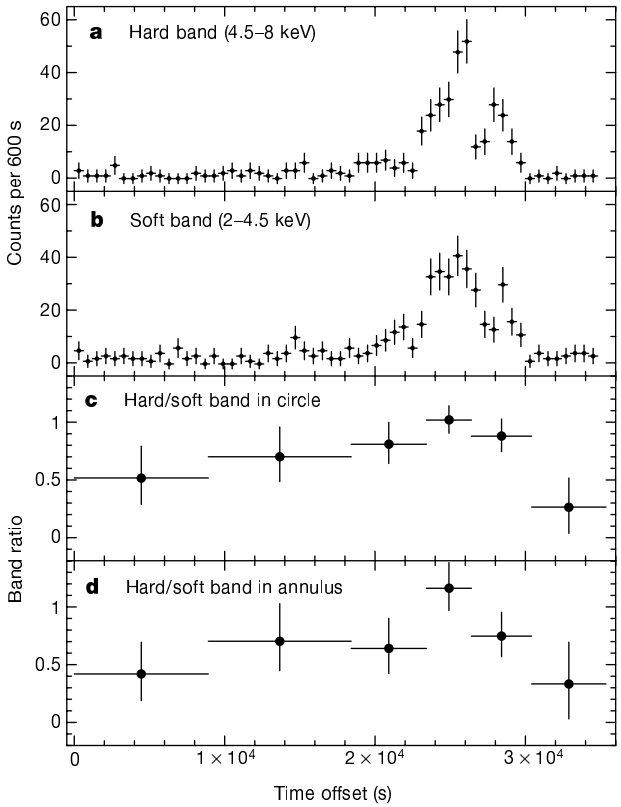

Figure 2 Light curves of the photon arrival times and band ratios from the direction of Sgr A* on 26–27 October 2000. **a**, Hard-band (4.5–8 keV) counts. **b**, Soft-band (2–4.5 keV) counts. **c**, Hard/soft band ratio within a circle of radius 1.5″. **d**, Hard/soft band ratio within an annulus of inner and outer radii 0.5″ and 2.5″, respectively. The *x* axis shows the time offset from the start of the observation at 26 October 2000 22:29 (UT). The data are shown with 1σ error bars. The single 2.8-hour period of flaring activity which we have detected so far during a total of 21 hours of observations yields a (poorly determined) duty cycle of approximately 1/8. Our continuing observations of this source with Chandra will permit us to refine this value. During the quiescent intervals at the beginning and end of this observation, the mean count rate in the 2–8-keV band was $(6.4 \pm 0.6) \times 10^{-3}$ counts s^{-1}, consistent with the count rate we measured in 1999, which was $(5.4 \pm 0.4) \times 10^{-3}$ counts s^{-1}. The detected count rate at the peak of the flare was 0.16 ± 0.01 counts s^{-1} within an extraction circle of radius 1.5″, but this is about 30% less than the true incident count rate owing to pile-up of X-rays in the detector during the 3.2-s integration time for each CCD (charge-coupled device) read out.

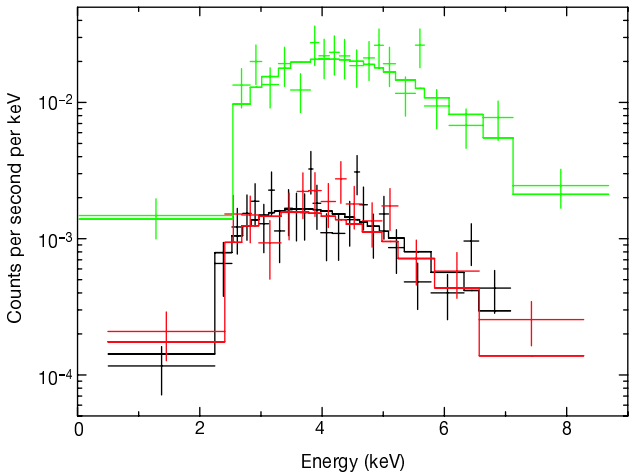

Figure 3 X-ray spectra of the Chandra source at the position of Sgr A*. The data are shown as crosses with vertical bars indicating the 1σ errors in the count rate and horizontal bars the energy range of each bin. The events have been grouped to yield 10 counts per bin. The counts in the 1999 (black) and 2000 (red) quiescent-state spectra were extracted using a source radius of 1.5″. A non-piled-up, peak flaring-state spectrum (green) was extracted from the wings of the point spread function, using an annulus with inner and outer radii of 0.5″ and 2.5″, during the time interval 23.7–26.3 ks after the start of the 2000 observation. The solid lines are the best-fit models for each spectrum, obtained by fitting an absorbed, dust-scattered, double power-law model to the three spectra simultaneously. The best-fit values and 90% confidence intervals for the model parameters are given in the last line of Table 1. The spectra are well-fitted using a single photon index for both quiescent spectra, a second photon index for the flaring spectrum, and a single column density for all three spectra. The column density from the simultaneous fits corresponds to a visual extinction $A_V = 29.6^{+5.0}_{-6.1}$ magnitudes, which agrees well with infrared-derived estimates of $A_V \approx 30$ magnitudes[7]; we thus find no evidence in our X-ray data of excess gas and dust localized around the supermassive black hole. This places an important constraint on the maximum contribution to the infrared spectrum of Sgr A* produced by local dust reprocessing of higher energy photons from the accretion flow. The spectral models used in ref. 6 did not account for dust scattering; hence a higher column density was needed to reproduce the low-energy cut-off via photoelectric absorption alone. We note that there is no sign of an iron Kα emission line in the flaring-state spectrum.

flaring source lies within 1/3″ of the radio position. These clusters contain up to a million solar masses of stars and stellar remnants[2]; hence it is rather improbable that there would be only one very unusual stellar X-ray source in the image and that it would be fortuitously superposed on Sgr A*. Furthermore, it is not clear that X-ray binaries can be easily formed or long endure near Sgr A*, given the high velocity dispersion and high spatial density of the stars in its deep gravitational potential well[6,12].

Strong, variable X-ray emission is a characteristic property of active galactic nuclei; factors of 2–3 variations on timescales ranging from minutes to years are typical for radio-quiet active galactic nuclei[11]. Moderate- to high-luminosity active galactic nuclei (that is, Seyfert galaxies and quasars) show a general trend of increasing variability with decreasing luminosity[13]. However, this trend does not extend to low-luminosity active galactic nuclei (LLAGN), which show little or no significant variability on timescales less than a day[14]. Assuming the X-ray flare is from Sgr A*, it is remarkable that this source—generally thought to be the nearest and least luminous example of accretion onto a central supermassive black hole—has shown a factor of 45 variation that is an order of magnitude more rapid than the fastest observed variation of similar relative amplitude by a radio-quiet active galactic nucleus of any luminosity class[15]. We note that flares of similar luminosity would be undetectable by Chandra in the nucleus of even the nearest spiral galaxy, M31. LLAGN emit $L_X \geq 10^{38}$ erg s^{-1} (ref. 14), so it should be kept in mind that the astrophysics of accretion onto even the LLAGN may differ substantially from that of Sgr A*. This makes Sgr A* a useful source for testing the theory of accretion onto supermassive black holes in galactic nuclei.

The faintness of Sgr A* at all wavelengths requires that the supermassive black hole be in an extremely quiet phase, either because the accretion rate is very low, or because the accretion flow is radiatively inefficient, or both[5]. A variety of theoretical scenarios, usually based on advective accretion models[16–19], jet–disk models[20], or Bondi–Hoyle models[21,22], have developed this idea. An important prediction of the advective accretion models is that the X-ray spectrum in the Chandra energy band should be dominated by thermal bremsstrahlung emission from hot gas in the outer regions of the accretion flow ($R \gtrsim 10^3 R_S$), but a region this large could not produce the rapid, large-relative-amplitude variations we have seen. Thus, the properties of the X-ray flare are inconsistent with the advective accretion flow models. The low luminosity and short timescales of this event are also inconsistent with tidal disruption of a star by a central supermassive black hole[23].

In all models, the radio-to-submillimetre spectrum of Sgr A* is cyclo-synchrotron emission from a combination of sub-relativistic and relativistic electrons (and perhaps positrons) spiralling around magnetic field lines either in a jet or in a static region within the inner $10 R_S$ of the accretion flow. The electron Lorentz factor inferred from the radio spectrum of Sgr A* is $\gamma_e \approx 10^2$. If the X-ray flare were produced via direct synchrotron emission, then the emitting electrons would need $\gamma_e \gtrsim 10^5$. For the 10–100 G magnetic field strengths predicted by the models, the cooling time of the particles would be ~1–100 s. Thus, the approximately 10-ks duration of the flare would require repeated injection of energy to the electrons. On the other hand, if the X-rays were produced via up-scattering of the submillimetre photons off the relativistic electrons, a process called synchrotron self-Comptonization (SSC), then $\gamma_e \approx 10^2$–10^3 would be required, and the cooling time would be of the order of hours, which is consistent with the duration of the flare. The rapid turn-off of the X-ray emission might then be attributed to the dilution of both photon and electron densities in an expanding plasma.

The X-ray spectra of radio-quiet quasars and active galactic nuclei are thought to be produced by thermal Comptonization of infrared-to-ultraviolet seed photons from a cold, optically thick, geometrically thin accretion disk by hot electrons in a patchy corona above the disk[13,24]. The X-ray spectra of these sources generally 'soften' (that is, become steeper and extend less strongly to higher energies) as they brighten[15]. In contrast, the extremely low luminosity of Sgr A* precludes the presence of a standard, optically thick accretion disk[5]; hence, the dominant source of seed photons would be the millimetre-to-submillimetre synchrotron photons.

The energy released by an instability in the mass accretion rate or by a magnetic reconnection event near the black hole would shock-accelerate the electrons, causing the synchrotron spectrum to intensify and to extend farther into the submillimetre band. Consequently, the Compton up-scattered X-ray emission would harden as the X-ray intensity increased, exactly as observed. We note that the millimetre-band spectrum of Sgr A* has been observed to harden during one three-week flare[25] and one three-day flare[26], as would be required by the current SSC models for Sgr A* (refs 20, 22).

To test the SSC models, we measured the flux density of Sgr A* at a wavelength of 3 mm with the Millimeter Array at the Owens Valley Radio Observatory, simultaneous with part of the 2000 Chandra measurement. Unfortunately, the available observing window (20:10–02:30 UT) preceded the X-ray flare (04:03–06:50 UT) by a few hours. The observed flux density of Sgr A* was 2.05 ± 0.3 Jy, consistent with previously reported measures[27,28]. Recently, a 106-day quasi-periodicity has been reported in the centimetre band from an analysis of 20 years of data taken with the Very Large Array (VLA)[29]. A weekly VLA monitoring program detected a 30% increase in the radio flux density of Sgr A* beginning around 24 October 2000 and peaking on 5 November 2000. This increase was seen at 2 cm, 1.3 cm, and 7 mm (R. McGary, J.-H. Zhao, W. M. Goss and G. C. Bower, personal communication). The timing of the X-ray flare and the rise in the radio flux density of Sgr A* suggests that there is a connection between the two events, providing additional indirect support for the association of the X-ray flare with Sgr A* and further strengthening the case that it was produced via either the SSC or direct synchrotron processes. Definitive evidence for these ideas will require detection of correlated variations in the radio-to-submillimetre and X-ray wavebands through future coordinated monitoring projects. □

Table 1 Spectral fits

Spectrum	N_H	Γ_q	Γ_f	χ^2/ν
1999 quiescent	$5.8^{+1.3}_{-1.4}$	$2.5^{+0.8}_{-0.7}$	...	19/22
2000 quiescent	$5.0^{+1.9}_{-2.3}$	$1.8^{+0.7}_{-0.9}$	...	7.6/12
2000 flaring	$4.6^{+2.0}_{-1.8}$	...	$1.0^{+0.8}_{-0.7}$	12/17
All	$5.3^{+0.9}_{-1.1}$	$2.2^{+0.5}_{-0.7}$	$1.3^{+0.5}_{-0.6}$	45/55

Best-fit parameter values and 90% confidence intervals for power-law models, corrected for photoelectric absorption and dust scattering[10]. N_H is the neutral hydrogen absorption column in units of 10^{22} H atoms cm^{-2}. Γ_q and Γ_f are the photon-number indices of the quiescent-state and peak flaring-state spectra ($N(E) \propto E^{-\Gamma}$). χ^2 is the value of the fit statistic for the best-fit model, and ν is the number of degrees of freedom in the fit. The parameter values for the spectrum marked 'All' were derived by fitting an absorbed, dust-scattered, double power-law model to the three spectra simultaneously (see text and Fig. 3).

Received 27 April; accepted 2 August 2001.

1. Richstone, D. *et al*. Supermassive black holes and the evolution of galaxies. *Nature* **395** (suppl. on optical astronomy) A14–A19 (1998).
2. Genzel, R., Pichon, C., Eckart, A., Gerhard, O. E. & Ott, T. Stellar dynamics in the Galactic Centre: proper motions and anisotropy. *Mon. Not. R. Astron. Soc.* **317**, 348–374 (2000).
3. Ghez, A. M., Morris, M., Becklin, E. E., Tanner, A. & Kremenek, T. The accelerations of stars orbiting the Milky Way's central black hole. *Nature* **407**, 349–351 (2000).
4. Lynden-Bell, D. & Rees, M. J. On quasars, dust and the Galactic Centre. *Mon. Not. R. Astron. Soc.* **152**, 461–475 (1971).
5. Melia, F. & Falcke, H. The supermassive black hole at the Galactic Center. *Annu. Rev. Astron. Astrophys.* **39**, 309–352 (2001).
6. Baganoff, F. K. *et al*. Chandra X-ray spectroscopic imaging of Sgr A* and the central parsec of the Galaxy. *Astrophys. J.* (submitted); also preprint astro-ph/0102151 at ⟨xxx.lanl.gov⟩ (2001).
7. Morris, M. & Serabyn, E. The galactic center environment. *Annu. Rev. Astron. Astrophys.* **34**, 645–702 (1996).
8. Menten, K. M., Reid, M. J., Eckart, A. & Genzel, R. The position of Sagittarius A*: accurate alignment of the radio and infrared reference frames at the Galactic Center. *Astrophys. J.* **475**, L111–L114 (1997).
9. Weisskopf, M. C., O'Dell, S. L. & van Speybroeck, L. P. Advanced X-Ray Astrophysics Facility (AXAF). *Proc. SPIE* **2805**, 2–7 (1996).

10. Predehl, P. & Schmitt, J. H. M. M. X-raying the interstellar medium: ROSAT observations of dust scattering halos. *Astron. Astrophys.* **293,** 889–905 (1995).
11. Mushotzky, R. F., Done, C. & Pounds, K. A. X-ray spectra and time variability of active galactic nuclei. *Annu. Rev. Astron. Astrophys.* **31,** 717–761 (1993).
12. Davies, M. B., Blackwell, R., Bailey, V. C. & Sigurdsson, S. The destructive effects of binary encounters on red giants in the Galactic Centre. *Mon. Not. R. Astron. Soc.* **301,** 745–753 (1998).
13. Nandra, K., George, I. M., Mushotzky, R. F., Turner, T. J. & Yaqoob, T. ASCA observations of Seyfert 1 galaxies. I. Data analysis, imaging, and timing. *Astrophys. J.* **476,** 70–82 (1997).
14. Ptak, A., Yaqoob, T., Mushotzky, R., Serlemitsos, P. & Griffiths, R. X-ray variability as a probe of advection-dominated accretion in low-luminosity active galactic nuclei. *Astrophys. J.* **501,** L37–L40 (1998).
15. Ulrich, M.-H., Maraschi, L. & Urry, C. M. Variability of active galactic nuclei. *Annu. Rev. Astron. Astrophys.* **35,** 445–502 (1997).
16. Narayan, R., Mahadevan, R., Grindlay, J. E., Popham, R. G. & Gammie, C. Advection-dominated accretion model of Sagittarius A*: evidence for a black hole at the Galactic center. *Astrophys. J.* **492,** 554–568 (1998).
17. Quataert, E. & Narayan, R. Spectral models of advection-dominated accretion flows with winds. *Astrophys. J.* **520,** 298–315 (1999).
18. Ball, G. H., Narayan, R. & Quataert, E. Spectral models of convection-dominated accretion flows. *Astrophys. J.* **552,** 221–226 (2001).
19. Blandford, R. D. & Begelman, M. C. On the fate of gas accreting at a low rate on to a black hole. *Mon. Not. R. Astron. Soc.* **303,** L1–L5 (1999).
20. Falcke, H. & Markoff, S. The jet model for Sgr A*: radio and X-ray spectrum. *Astron. Astrophys.* **362,** 113–118 (2000).
21. Melia, F. An accreting black hole model for Sagittarius A*. II: A detailed study. *Astrophys. J.* **426,** 577–585 (1994).
22. Melia, F., Liu, S. & Coker, R. Polarized millimeter and submillimeter emission from Sagittarius A* at the Galactic center. *Astrophys. J.* **545,** L117–L120 (2000).
23. Rees, M. J. Tidal disruption of stars by black holes of 10^6–10^8 solar masses in nearby galaxies. *Nature* **333,** 523–528 (1988).
24. Haardt, F., Maraschi, L. & Ghisellini, G. X-ray variability and correlations in the two-phase disk-corona model for Seyfert galaxies. *Astrophys. J.* **476,** 620–631 (1997).
25. Tsuboi, M., Miyazaki, A. & Tsutsumi, T. in *The Central Parsecs of the Galaxy* (ed. Falcke, H. *et al.*) Vol. 186, 105–112 (ASP Conf. Ser., Astronomical Society of the Pacific, San Francisco, 1999).
26. Wright, M. C. H. & Backer, D. C. Flux density of Sagittarius A at λ = 3 millimeters. *Astrophys. J.* **417,** 560–564 (1993).
27. Serabyn, E. *et al.* High frequency measurements of the spectrum of SGR A*. *Astrophys. J.* **490,** L77–L81 (1997).
28. Falcke, H. *et al.* The simultaneous spectrum of Sagittarius A* from 20 centimeters to 1 millimeter and the nature of the millimeter excess. *Astrophys. J.* **499,** 731–734 (1998).
29. Zhao, J.-H., Bower, G. C. & Goss, W. M. Radio variability of Sagittarius A*—a 106 day cycle. *Astrophys. J.* **547,** L29–L32 (2001).
30. Reid, M. J. The distance to the center of the Galaxy. *Annu. Rev. Astron. Astrophys.* **31,** 345–372 (1993).

Acknowledgements

We thank M. Begelman for useful comments. This work has been supported by a grant from NASA.

Correspondence and requests for materials should be addressed to F.K.B. (e-mail: fkb@space.mit.edu).

How 'spin ice' freezes

J. Snyder*, J. S. Slusky†, R. J. Cava† & P. Schiffer*

* *Department of Physics and Materials Research Institute, Pennsylvania State University, University Park, Pennsylvania 16802, USA*
† *Department of Chemistry and Princeton Materials Institute, Princeton University, Princeton, New Jersey 08540, USA*

The large degeneracy of states resulting from the geometrical frustration of competing interactions is an essential ingredient of important problems in fields as diverse as magnetism[1], protein folding[2] and neural networks[3]. As first explained by Pauling[4], geometrical frustration of proton positions is also responsible for the unusual low-temperature thermodynamics of ice and its measured 'ground state' entropy[5]. Recent work has shown that the geometrical frustration of ice is mimicked by $Dy_2Ti_2O_7$, a site-ordered magnetic material in which the spins reside on a lattice of corner-sharing tetrahedra where they form an unusual magnetic ground state known as 'spin ice'[6–13]. Here we identify a cooperative spin-freezing transition leading to the spin-ice ground state in $Dy_2Ti_2O_7$. This transition is associated with a very narrow range of relaxation times, and represents a new form of spin-freezing. The dynamics are analogous to those associated with the freezing of protons in ice, and they provide a means through which to study glass-like behaviour and the consequences of frustration in the limit of low disorder.

In the ground state of ordinary hexagonal ice (I_h), neighbouring oxygen ions are connected through a hydrogen bond (Fig. 1a), and each hydrogen ion (proton) is situated closer to one or the other of its oxygen nearest-neighbours. This situation was codified by Pauling[4] as the "ice rules": that there should be a proton between each oxygen pair and that it should be localized near one or the other oxygen site. As each oxygen ion has four oxygen nearest-neighbours, the ice rules require that two of the neighbouring protons will be close to, and two will be far from, any particular oxygen ion. There is a six-fold degeneracy of protonic states that obey this rule for any given oxygen site, and a macroscopic degeneracy of allowed states in an extended crystal. Although the proton positions are dynamic at high temperatures owing to mobile protonic point defects (for example, two or zero interstitial protons between oxygen sites), the dynamics slow substantially with decreasing temperature, and the protons effectively freeze into a disordered configuration below $T \approx 100$ K (refs 14, 15). The metastable nature of this frozen state leads to the observation of a 'practical' ground-state entropy, associated with the random configuration of the protons as $T \rightarrow 0$, which is in almost exact agreement with that expected from the ice rules[15,16].

The statistical mechanics of the ice rules may be mimicked by certain rare-earth magnets with the pyrochlore structure[6]. In such a spin-ice material, the magnetic rare-earth ions are situated on a lattice of corner-sharing tetrahedra and their spins are constrained by crystal field interactions[11,17] to point either directly towards or directly away from the centres of the tetrahedra (Fig. 1b). Dipole and ferromagnetic exchange interactions between the spins require that, on each tetrahedron, two spins point inward and two point outward. This situation exactly mirrors the frustration associated with the ice rules, and leads to the same large degeneracy of states[10–13]. The spin-ice state has been realized experimentally[9,11] in $Dy_2Ti_2O_7$, in which the magnetic specific heat integrated from zero temperature yields a measured ground-state entropy in exact agreement with the theoretical prediction for the ice rules and experimental results for ice[5,15,16].

In order to examine the development of the magnetic ground state of spin ice, we study the magnetization (M) and the resultant d.c. susceptibility ($\chi_{dc} = dM/dH$, where H is the applied magnetic field) as well as the real and imaginary parts (χ' and χ'') of the a.c. susceptibility (χ_{ac}) of polycrystalline $Dy_2Ti_2O_7$. The calorimetric measurements suggest spin-freezing into a non-equilibrium state[9,10], but we find that χ_{dc} increases monotonically with decreas-

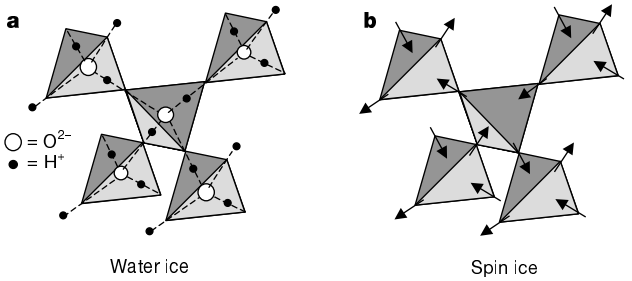

Figure 1 Schematic representation of frustration in water ice and spin ice. **a**, In water ice, each hydrogen ion is close to one or the other of its two oxygen neighbours, and each oxygen must have two hydrogen ions closer to it than to its neighbouring oxygen ions. **b**, In spin ice, the spins point either directly toward or away from the centres of the tetrahedra, and each tetrahedron is constrained to have two spins pointing in and two pointing out.

